ELSEVIER

Chemical Engineering Journal 135S (2008) S237–S241

Chemical Engineering Journal

www.elsevier.com/locate/cej

Parametric investigation of rate enhancement during fast temperature cycling of CO oxidation in mircroreactors

Søren Jensen [a,*], Sune Thorsteinsson [a], Ole Hansen [a], Ulrich J. Quaade [b]

[a] *MIC – Department of Micro and Nanotechnology, Technical University of Denmark, Building 345 East, 2800 Kgs. Lyngby, Denmark*
[b] *Center for Individual Nanoparticle Functionality (CINF), Department of Physics, NanoDTU, Technical University of Denmark, Building 312, 2800 Kgs. Lyngby, Denmark*

Abstract

A new microreactor that allows investigation of the effects of temperature oscillations at frequencies 10 times higher than in previous systems is presented. As an example, we investigate CO oxidation over a supported Pt catalyst subjected to a fast forced oscillation of the reactor temperature and confirm earlier findings of reaction rate enhancements. The enhancement is shown to increase at high frequencies. Varying the conversion and temperature oscillation amplitude is shown to have a large effect on the rate enhancement, and a large interaction between the two parameters is detected. For the best parameter setting, reaction rates 70% higher than during slow steady-state-like oscillations are observed.

Keywords: Microreactor; Temperature cycling; Unsteady-state processing

1. Introduction

Subjecting catalytic chemical reactions to periodically varying operation conditions has shown to have a number of beneficiary effects, including increase of the reaction rate, improvement of the selectivity, and reduction of the catalyst deactivation [1]. Initially, the majority of the research was directed towards studies of the effect of varying reactant concentrations, since the large thermal mass of conventional reactors prohibited investigations of the effect of temperature oscillations at relevant frequencies. Recently, however, microfabricated reactors (microreactors) [2] capable of performing fast temperature oscillations have become available, and we can now explore a new, vast parameter space, which has previously been inaccessible. The temperature oscillation offset, amplitude, and frequency are expected to influence catalytic reactions [3], and the parameter space contains possibilities for obtaining higher reaction rates and thus more efficient chemical processing than in steady state. Rate enhancement during CO oxidation has been demonstrated in stainless steel reactors [4,5], as well as in silicon reactors [6], but a further exploration of the parameter space is needed to help elucidate the underlying mechanisms. To perform such exploration, we present a new reactor with integrated heating, temperature measurement, and mass spectrometer interface. The use of integrated heating provides access to frequencies 10 times higher than what could be obtained in our previously reported reactors [6].

As an example, we study CO oxidation over a supported platinum catalyst. To obtain an initial understanding of the effect of the different parameters and their interactions, we use design of experiments (DOE) [7].

2. Experimental setup

2.1. Microreactor

To investigate the effects of fast temperature oscillations, we use a microreactor made of silicon since it provides excellent heat conduction necessary for realizing fast temperature oscillations and can withstand elevated temperatures. Furthermore, the multitude of available processing tools developed in the semiconductor industry provides vast possibilities for integration of sensors and actuators on the reactor chip. In particular, the reactor is equipped with a direct mass spectrometer interface for fast gas detection as well as a nickel silicide thin film heater and a resistor thermometer for fast and accurate control of the reaction temperature. Fig. 1 shows the reactor seen from the front and the back.

The reactor chamber, in/outlet channels, and mass spectrometer interface are etched in the silicon using deep reactive ion

* Corresponding author. Tel.: +45 45 25 63 32; fax: +45 45 88 77 62.
E-mail address: sj@mic.dtu.dk (S. Jensen).

1385-8947/$ – see front matter © 2007 Elsevier B.V. All rights reserved.
doi:10.1016/j.cej.2007.07.031

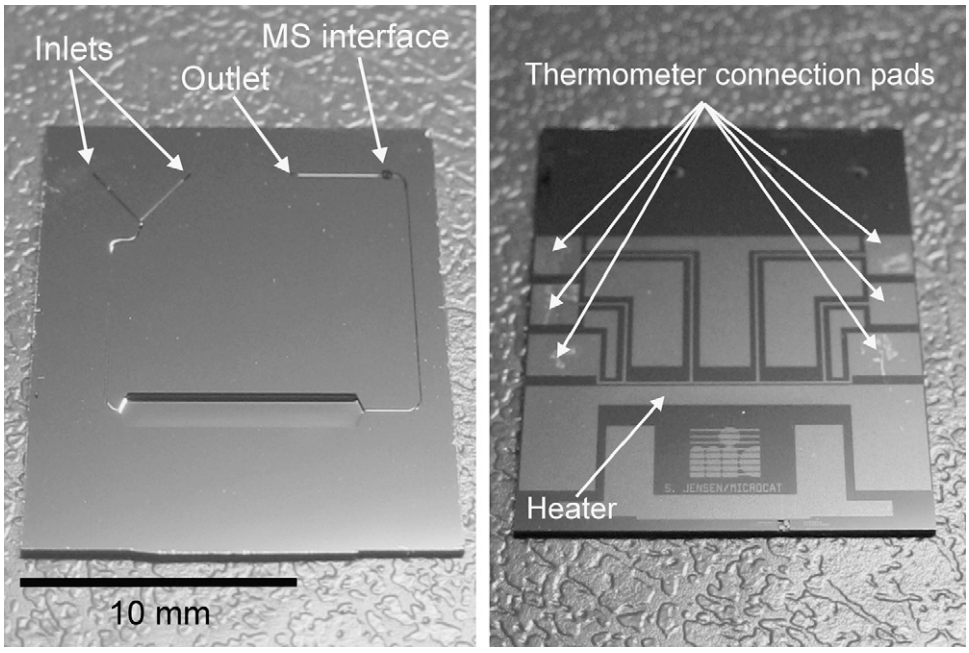

Fig. 1. Microreactor seen from the front (left) and back (right).

etching (DRIE) [8]. First, the in/outlet holes and the mass spectrometer interface are etched in the back of the substrate to a depth of about 30–40 μm. Thereafter, the substrate is turned around and the reactor chamber and channels are etched from the front side until the channels meet the in/outlet holes.

The mass spectrometer interface [9] is a very narrow (approximately, 2–4 μm in diameter and 30–40 μm long) through-hole with a flow resistance large enough that the flow through the hole is of the order 10^{-9} mol/s, which is suitable for a mass spectrometer, when the reactor is at atmospheric pressure and the mass spectrometer at 10^{-6} Torr.

The integrated heater and thermometer are fabricated by reacting a deposited nickel layer with an underlying poly-silicon layer to form a 200 nm thick nickel-silicide (NiSi) layer in a thermal anneal process. The NiSi layer is electrically insulated from the silicon substrate by a 200 nm thick SiO_2 layer thermally grown on the substrate prior to the poly-silicon deposition. The room temperature resistance of the thermometer and heater is 107 Ω and 12 Ω, respectively.

The reactors are fabricated on 4 in. silicon substrates each holding 16 reactors. After the microfabrication, the reactors are separated and handled individually. The catalyst is placed in the reactor by first depositing an AlOOH gel which is subsequently impregnated with $Pt(acac)_2$, as described in [6]. The reactor is calcined in air at 400 °C to obtain porous alumina with dispersed platinum nanoparticles. The final catalyst consists of 2.5 mg support with 5 wt% platinum, and has a BET area of 130 m^2/g. After preparation of the catalyst, the reactor is sealed with a Pyrex lid using anodic bonding.

2.2. Interface

During measurements, the reactor is placed in an aluminium interface block providing electrical and gas connections as shown in Fig. 2. The reactor is pressed against a set of Viton *o*-rings to ensure proper sealing, whereafter spring-loaded probes providing electrical connections to heater and thermometer are raised towards the underside of the reactor.

2.3. Temperature oscillation and measurement

During the experiments, the reactor temperature is varied by applying a sinusoidally varying voltage,

$$V(t) = V_0 + v\sin(2\pi ft), \tag{1}$$

across the heater element of resistance R_H, where V_0 is the dc offset, v the ac amplitude, and f the oscillation frequency. The reactor temperature is approximately proportional to the dissipated power, $P = V\,2/R_H$, and one would therefore expect temperature oscillations at both the drive frequency and twice the drive frequency. The contribution at twice the drive frequency, however, is very small as long as $v \ll V_0$, and we expect the

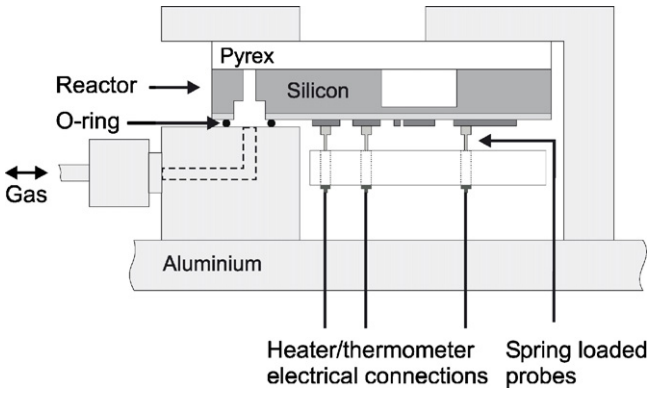

Fig. 2. Microreactor placed in interface block.

temperature to vary around an offset temperature according to

$$T(t) = T_0 + A\sin(2\pi ft), \quad (2)$$

where T_0 is the offset temperature, and A the temperature oscillation amplitude.

The temperature in the reactor is measured by measuring the resistance of a NiSi strip and recorded using LabView software capable of sampling up to 14 times/s. The voltages are adjusted manually, and it is possible to realize accurate temperature oscillations within a precision 0.5 °C. The resistance of NiSi varies linearly with temperature according to the relationship

$$R(T) = R_0(1 + \alpha(T - T_0)), \quad (3)$$

where α is the temperature coefficient of resistance (TCR), and T_0 and R_0 are arbitrary reference temperature and the corresponding resistance. The TCR has been determined to be $4.5 \times 10^{-3}\,K^{-1}$ by calibration in a furnace. The thermometer has six connections along its length allowing for four-point measurement of the resistance of any third of the thermometer or of the entire thermometer length.

The thermometer is located 100 μm laterally away from the heater element on a thin SiO_2/Si membrane, and thus provides measurements with delays on the order of milliseconds. The reactor chamber is separated from the heater by approximately 200 nm silicon dioxide and 30 μm of silicon, which yields even shorter heat transfer times.

3. Data analysis

We study oxidation of CO over a supported Pt catalyst,

$$CO + \tfrac{1}{2}O_2 \rightarrow CO_2, \quad (4)$$

as a model reaction. The feed gas used consists of 5% CO, 2.5% O_2, 2.5% Ar, and 90% He as carrier gas. The Ar is non-reactive and is used for calibration since the flow through the mass spectrometer interface is temperature dependent [10]. Blind-activity measurements in an empty reactor and in one with the support matrix without catalyst show no conversion.

Since the reaction rate depends exponentially on temperature, the mean reaction rate during an oscillation period will always be larger than the reaction rate at the mean temperature. To measure reaction rate increases beyond this trivial increase, we calculate a reaction rate ratio, Φ, between the measured, time-averaged reaction rate at the frequency in question and the time-average obtained at 0.02 Hz, where the reactor follows steady-state behaviour. The slow oscillation is taken at the same oscillation offset and amplitude. $\Phi = 1$ therefore corresponds to the trivial rate increase due to the oscillation while $\Phi > 1$ corresponds to genuine rate enhancement. There are uncertainties associated with the measured Φ, originating from drift in the system and random fluctuations of e.g. flow controllers. The uncertainties are minimized by careful system warm-up and time averaging, and by repeated measurements at different constant parameter settings, they are estimated to be less than 5% in total.

4. Thermal reactor characterization

By using an integrated heater, it is possible to explore higher frequencies than previously, but the use of a simple strip heater gives rise to thermal gradients along the reactor. The temperature decreases towards the reactor edges, and during experiments, it is therefore the average reaction rate from a temperature distribution that will be measured, and not the rate at a single, well-defined temperature.

By using the three-segment thermometer, this gradient and any possible frequency dependencies, which could obscure rate enhancement measurements, are investigated.

The temperature of the reactor was measured using the central third of the thermometer as well as one of the outer thirds during steady state and dynamic operation. In general, the edge regions are colder than the center, as expected.

In steady state, the ratio between the edge and center temperatures (measured in °C) decreases approximately linearly from unity at room temperature to 0.9 at 200 °C.

During dynamic operation, the temperature oscillation amplitude is smaller in the outer regions than in the center. As an example, an oscillation of the center temperature between 160 °C and 140 °C results in a temperature oscillation between 147 °C and 130 °C in the edge regions. Increasing the frequency from 0.01 to 0.5 Hz decreases the oscillation amplitude by 0.6 °C but does not change the offset. We thus do not expect the fact that we measure the response from a temperature distribution to affect findings of rate enhancement. The temperature distribution is relatively insensitive to frequency increases, and the 0.6 °C decrease in amplitude would not result in rate increases.

Before planning experiments, the extent of the accessible part of the oscillation parameter space was investigated. In steady-state operation, the maximum obtainable reactor temperature was 350 °C at a power of 26 W. In oscillation mode, the reactor sustained a 1.2 Hz oscillation at an offset of 183 °C and with an amplitude of 32.5 °C. This corresponds to heating/cooling rates of more than 150 °C/s, which is more than a 10-fold increase compared to our previously reported reactors [6].

5. CO oxidation experiments

The relevant parameters to investigate are the feed gas flow rate, Q, the temperature oscillation offset, T_0, amplitude, A, and frequency, f. The aim of this investigation is to introduce the flow as a parameter and to investigate the responses at higher frequencies than previously.

From earlier investigations [6], we know that the rate enhancement increases with frequency, and in this investigation, we therefore fix the frequency at 1 Hz to get as large a response as possible and at the same time stay within safe limits. In the presentation of the results, we will refer to the temperature in the middle third of the reactor.

5.1. Offset and flow rate

To begin with, the effects of varying the offset and flow rate are investigated. The volume of the reactor chamber is

Table 1
Rate ratios at 1 Hz for different offsets, T_0, and flow rates, Q

T_0 (°C)	$Q = 3\,mm^3/s$	$Q = 16\,mm^3/s$
140	1.21 (4%)	–
160	1.19 (20%)	1.18 (4%)
180	1.05 (62%)	1.19 (32%)

The values in brackets are the conversions.

$V = 3.6\,mm^3$, not taking the volume of the catalyst support into account. The flow rates used are in the range 3–16 mm^3/s at standard conditions, giving residence times from 1 to 0.2 s. By visual inspection, the catalyst support is estimated to take up less than half of the reactor volume.

Table 1 shows the reaction rate ratio for different offsets and flow rates with the degree of CO conversion listed in brackets. The frequency is 1 Hz and the amplitude 10 °C in all measurements.

The estimated 5% uncertainty means that the error is on the second decimal, and within the parameter range investigated, the only parameter combination that yields a ratio significantly different from 1.2 is that where the flow set to its "low" setting and the offset to its "high" setting. This is also the setting at which the CO conversion is highest, namely 62%. The rate ratio seems relatively insensitive to variations in the flow and offset unless it results in a large degree of conversion. The conversion, X, is the relative amount of CO converted to CO_2, and can be written as

$$X = \frac{r(T)}{\dot{n}}, \tag{5}$$

where $r(T)$ is the (temperature dependent) molar reaction rate, $\dot{n}$ the molar flow rate of CO. Since the reaction rate increases with offset temperature, it seems possible to simplify the following investigations by using the conversion as a combined parameter reflecting the flow and the offset.

5.2. Conversion and amplitude

Having collapsed the flow rate and offset into a single parameter, the conversion, we now investigate the effect of varying the oscillation amplitude together with the conversion.

Table 2 shows rate ratios at 1 Hz for different conversions and amplitudes. As expected from the previous experiments, we see the highest reaction rate ratios at low conversions. Varying the amplitude seems to have a much larger effect at low conversion than at high conversion. At low conversion, the reaction rate ratio increases from 1.2 to 1.7 when increasing the amplitude from 10 to 20 °C. At high conversion the corresponding increase is only from 1.07 to 1.10, which is close to being within the uncertainty of the experiment. The conversion was allowed to vary some

Table 2
Rate ratios at 1 Hz for different conversions, X, and amplitudes, A

X	$A = 10\,°C$	$A = 20\,°C$
Low (4–16%)	1.20	1.70
High (55–56%)	1.07	1.10

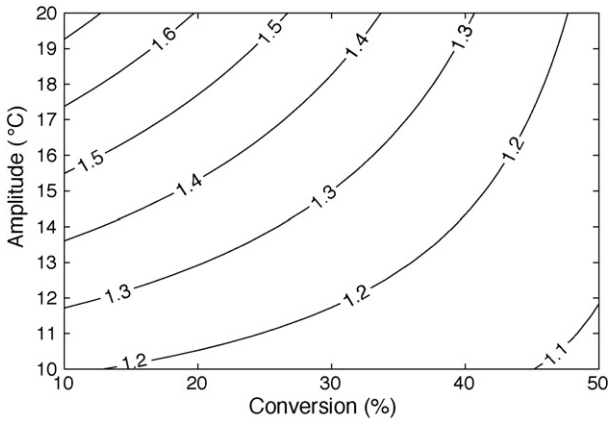

Fig. 3. Contour plot of the fitted reaction rate ratio as a function of conversion and temperature oscillation amplitude.

at its "low" setting, but from the data in Table 1, this is only expected to have a minimal influence on the rate ratio.

It seems from Table 2 that there is a substantial interaction between the two parameters. To get a quantitative indication of the interaction, the data is fitted with a simple first-order model including an interaction term. The fit is made using scaled and centered parameters X and A, which are parameters resulting from mapping the regular parameter intervals $A \in [10\,°C; 20\,°C]$ and $X \in [10\%; 55\%]$ (using the average at low conversion) onto $[-1; 1]$ intervals. In this way, the coefficients of the terms in the fit can be directly compared without having to take into account any scaling due to the specific units chosen for the parameters. The fitting yields the following relationship

$$\Phi = 1.300 - 0.174\hat{X} + 0.153\hat{A} - 0.112\hat{X}\hat{A}, \tag{6}$$

and it is noted that all the three coefficients are of the same order of magnitude. The fitted surface is shown with a contour plot in Fig. 3, where the interaction is visible as a curvature of the lines of constant reaction rate ratio.

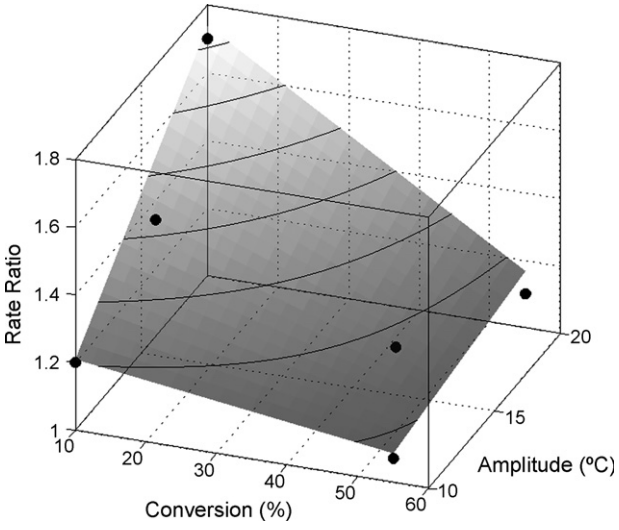

Fig. 4. The rate ratio as a function of conversion and temperature oscillation amplitude.

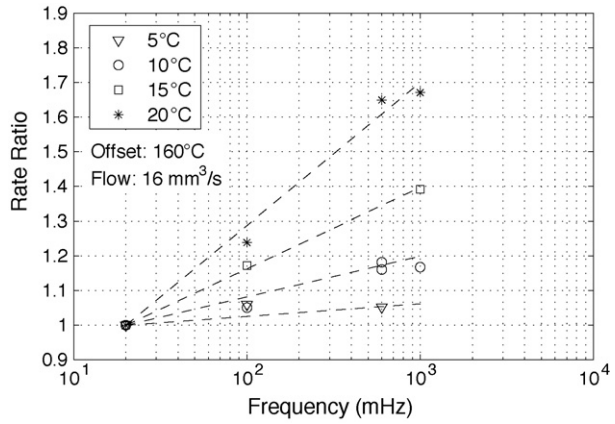

Fig. 5. The rate ratio as a function of frequency for four different amplitudes at low conversion.

The fit is based on a minimum number of points, but measurements taken later at 15 °C amplitude and 12% and 46% conversion yield rate ratios of 1.40 and 1.14, respectively, which correspond well to the ratios of 1.43 and 1.16 one gets by inserting numbers in (6). The fit is illustrated in Fig. 4, which shows a 3D-plot of the data along with the fitted surface.

Fig. 5 shows measurements of the rate ratio as a function of frequency for four different amplitudes at low conversion ($X < 16\%$), constant offset ($T_0 = 160\,^{\circ}\mathrm{C}$), and constant flow rate ($Q = 16\,\mathrm{mm}^3/\mathrm{s}$). It is noted that the rate ratio increases with frequency into the recently accessible part of the parameter space above 0.1 Hz, and the increase of the rate ratio with temperature oscillation amplitude seen in Table 2 is confirmed with measurements at intermediate amplitudes and frequencies.

6. Conclusion

We have presented a new reactor that allows investigation of the effects of temperature oscillations at frequencies 10 times higher than in previous systems. The temperature distribution in the reactor has been shown to be independent of the applied oscillation frequency, but a more homogeneous temperature distribution would be desirable in future reactors.

We have investigated CO oxidation over a supported Pt catalyst subjected to a fast forced oscillation of the reactor temperature. Earlier findings of reaction rates larger than those found during slow steady-state-like oscillations have been confirmed, and the increase of the rate enhancement with frequency has been found to continue in the high-frequency part of the parameter space accessible with this reactor type.

Within the parameter range investigated, the effects of varying the flow rate and temperature oscillation offset can be ascribed to a variation in the degree of CO conversion.

The effects of varying the conversion and temperature oscillation amplitude have been investigated and strong interaction effects have been found. To get large reaction rate enhancement, one must ensure sufficiently low conversion combined with high oscillation amplitude and high frequency. The last two requirements place high demands on the mechanical stability and the heating and cooling rates of the reactor.

Acknowledgements

S. Jensen is funded by the Danish Research Council for Technology and Production Sciences (FTP). Center for Individual Nanoparticle Functionality is sponsored by the Danish National Research Foundation.

References

[1] P. Silveston, R.R. Hudgins, A. Renken, Periodic operation of catalytic reactors—introduction and overview, Catal. Today 25 (2) (1995) 91–112.
[2] Klavs F. Jensen, Microreaction engineering—is small better? Chem. Eng. Sci. 56 (2) (2001) 293–303.
[3] P.L. Silveston, R.R. Hudgins, Periodic temperature forcing of catalytic reactions, Chem. Eng. Sci. 59 (19) (2004) 4043–4053.
[4] J. Brandner, M. Fichtner, K. Schubert, M. Liauw, G. Emig, A new microstructure device for fast temperature cycling for chemical reactions, in: Microreaction Technology: IMRET 5; Proceedings of the 5th International Conference, Berlin, Springer Verlag, 2001, pp. 164–174.
[5] J.J. Brandner, G. Emig, M.A. Liauw, K. Schubert, Fast temperature cycling in microstructure devices, Chem. Eng. J. 101 (1–3) (2004) 217–224.
[6] Heine A. Hansen, Jakob L. Olsen, Søren Jensen, Ole Hansen, Ulrich J. Quaade, Rate enhancement in microfabricated chemical reactors under fast forced temperature oscillations, Catal. Commun. 7 (5) (2006) 272–275.
[7] D.C. Montgomery, Design and Analysis of Experiments, Wiley, New York, 1997.
[8] A.M. Hynes, H. Ashraf, J.K. Bhardwaj, J. Hopkins, I. Johnston, J.N. Shepherd, Recent advances in silicon etching for MEMS using the ASE(TM) process, Sens. Actuators A 74 (1–3) (1999) 13–17.
[9] U.J. Quaade, S. Jensen, O. Hansen, Microsystem with integrated capillary leak to mass spectrometer for high-sensitivity temperature programmed desorption, Rev. Sci. Instrum. 75 (2004) 3345–3347.
[10] Ulrich J. Quaade, Søren Jensen, Ole Hansen, Fabrication and modelling of narrow capillaries for vacuum system gas inlets, J. Appl. Phys. 97 (2005) 44906.